ChemComm

Selective Dimerization of a Trinuclear Mixed-Metal Sandwich Complex: Construction of an Axially Chiral Metal Skeleton

Journal:	*ChemComm*
Manuscript ID	CC-COM-07-2021-003719.R1
Article Type:	Communication

ChemComm

COMMUNICATION

Selective Dimerization of a Trinuclear Mixed-Metal Sandwich Complex: Construction of an Axially Chiral Metal Skeleton

Received 00th January 20xx,
Accepted 00th January 20xx

DOI: 10.1039/x0xx00000x

www.rsc.org/

Hiroshige Yamaura, Koji Yamamoto, and Tetsuro Murahashi*

Certain metal sandwich complexes undergo dimerization through metal–metal bond formation. Here we found that reductive dimerization of the mixed metal Pd_2Pt or $PdPt_2$ sandwich complexes proceeds through selective Pt–Pt bond formation. Restricted rotation at the Pt–Pt bond of the $PdPt_2$ dimer gave a unique axially chiral structure derived from the heterometal arrangement in a mixed metal cluster.

The redox behaviour of organometallic sandwich complexes such as metallocenes has attracted much attention because of their usefulness as the redox reagents[1-7] or the redox-responsive components in functional materials.[8-10] In some cases, the redox processes of sandwich complexes accompany molecular transformations involving metal–metal bond formation[11-15] or ligand-ligand C–C coupling.[15,16] For example, d^5 metallocenes such as osmocenium give a metal–metal bonded dimer through bending of the sandwich structure (Scheme 1a),[11] although ferrocenium stands stably in its monomeric form.[1] More recently, our group reported that the triangular Pd_3 sandwich complexes of cycloheptatrienyl[17-19] or cycloheptatriene[14] showed the metal–metal bond forming dimerization upon one-electron reduction (Scheme 1b).[14] In the case of the Pd_3 sandwich complexes, each metal atom which is locating beneath the rim of the carbocyclic ligands is not well covered sterically by the ligands, that is advantageous for the purpose of the metal–metal bond forming dimerization without bending of the sandwich structure, as seen in the structure of the Pd_3 dimer **1** (Scheme 1b). It is of interest to verify which of possible three types of dimerization products, namely M–M, M–M', and M'–M' coupling products, is formed by reduction of a mixed metal MM'_2 sandwich complex (Scheme 1c). The three patterns of the arrangement of M and M' in the bi-triangle metal skeleton could give either chiral or achiral structure when the rotation at the metal–metal bond connecting two monomer units is restricted. Here we report the selective dimerization of a triangular Pd_2Pt or $PdPt_2$ sandwich complex through Pt–Pt bond formation. The restricted rotation at the newly formed Pt–Pt bond of the $PdPt_2$ dimer gives a unique axially chiral structure derived from the inorganic mixed metal arrangement in a metal cluster.

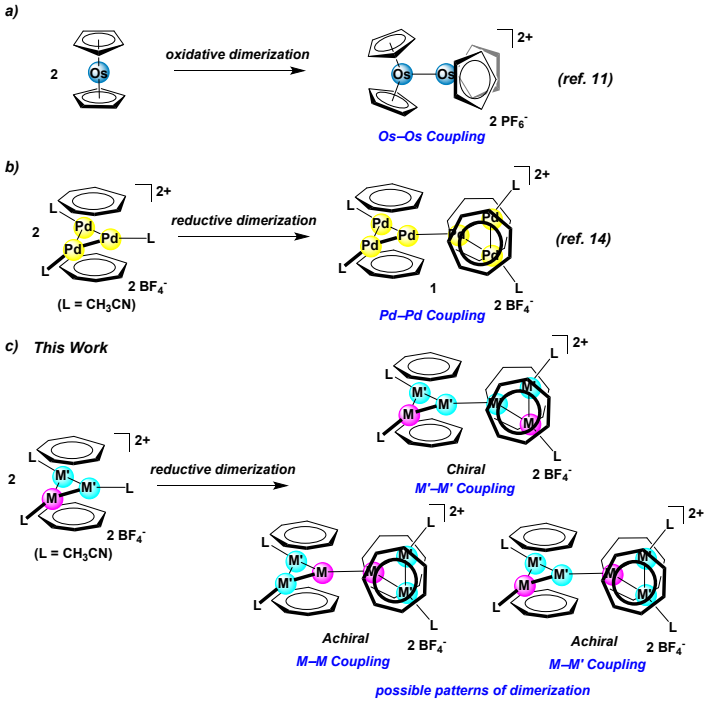

Scheme 1. The metal–metal bond forming dimerization of sandwich complexes.

The bis-cycloheptatrienyl sandwich complexes of mixed metal Pd_2Pt and $PdPt_2$ triangles, $[Pd_2Pt(\mu_3\text{-}C_7H_7)_2(CH_3CN)_3][BF_4]_2$ (**2**) and $[PdPt_2(\mu_3\text{-}C_7H_7)_2(CH_3CN)_3][BF_4]_2$ (**3**), were prepared according to our previous synthesis.[19] The ^1H NMR monitoring experiments of the reductive transformation of the orange monomer **2** with cobaltocene (1 equiv) in CD_3CN at room temperature showed that the dark purple dimer $[Pd_4Pt_2(\mu_3\text{-}C_7H_7)_4(CH_3CN)_4][BF_4]_2$ (**4**) was formed smoothly in 94% yield after 3 h (Scheme 2). On the other

Department of Chemical Science and Engineering, School of Materials and Chemical Technology, Tokyo Institute of Technology, O-okayama, Meguro-ku, Tokyo, 152-8552, Japan. E-mail: mura@apc.titech.ac.jp; Fax: +81 3 5734 2139; Tel: +81 3 5734 2148

† Electronic Supplementary Information (ESI) available: Experimental details of the preparation and characterization. CCDC 2094329-2094332. See DOI: 10.1039/x0xx00000x

hand, the reduction of the brown monomer **3** with cobaltocene (1 equiv) in CD_3CN afforded the dark brown dimer $[Pd_2Pt_4(\mu_3\text{-}C_7H_7)_4(CH_3CN)_4][BF_4]_2$ (**5**) only slowly: i.e., approximately a half amount of **3** was consumed after 1 h, but the yield of **5** was 10%, and then the dimer **5** was produced gradually (47% yield after 2 days), where any sign of the formation of other dimerization products could not be detected by ^1H NMR monitoring experiments. The reaction profile for the formation of **5** indicated that an unidentified intermediate is formed initially. The dimers **4** and **5** were isolated in 75% and 46% yield, respectively (Scheme 2).

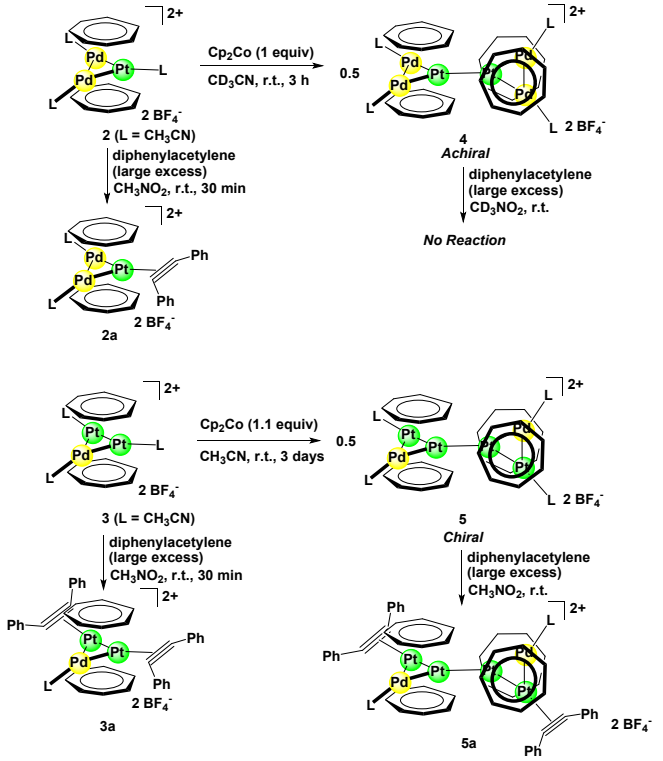

Scheme 2. Reductive dimerization of the Pd_2Pt or $PdPt_2$ sandwich cluster, and their alkyne binding behaviour.

The structure of **4** was determined by X-ray structure analysis (Figure 1). The Pd_2Pt triangle is connected through the Pt1–Pt2 bond (2.6793(3) Å) which is in the range of normal Pt–Pt bond, and actually shorter than other Pd–Pd (2.7034(7) Å; 2.6850(7) Å) and Pd–Pt bonds(2.7931(6) Å; 2.8449(6) Å) of the Pd_2Pt triangles in **4**. The two Pd_2Pt triangles are almost perpendicular with each other (the dihedral angle = 89.7°). As a result, the dimer **4** is in pseudo-D_{2d} symmetry, giving an achiral dimeric structure. On the other hand, it was difficult to determine the structure of **5** through X-ray structure analysis due to the positional disorder of Pd and Pt atoms. For discrimination of the Pd and Pt atoms in the crystalline state, we then thought to introduce certain ligands selectively at the Pt sites of **5**. We found that diphenylacetylene could be selectively introduced to the Pt sites[18] in **2**, **3**, and **5**, while no binding of diphenylacetylene was observed for **4** (Scheme 2). Recrystallization of $[Pd_2Pt(\mu_3\text{-}C_7H_7)_2(PhC{\equiv}CPh)(CH_3CN)_2][BF_4]_2$ (**2a**) or $[PdPt_2(\mu_3\text{-}C_7H_7)_2(PhC{\equiv}CPh)_2(CH_3CN)][BF_4]_2$ (**3a**) afforded a crystal of $[Pd_2Pt(\mu_3\text{-}C_7H_7)_2(PhC{\equiv}CPh)(CH_3CN)(BF_4)][BF_4]$ (**2a'**) or $[PdPt_2(\mu_3\text{-}C_7H_7)_2(PhC{\equiv}CPh)_2(H_2O)][BF_4]_2$ (**3a'**) (Figure 2), where acetonitrile ligands are eliminated during the recrystallization. It was confirmed that diphenylacetylene selectively coordinated to the Pt sites in the monomeric complex **2a'** or **3a'**. Recrystallization of the diphenylacetylene adduct of the dimer $[Pd_2Pt_4(\mu_3\text{-}C_7H_7)_4(\text{diphenylacetylene})_2(CH_3CN)_2][BF_4]_2$ (**5a**) gave a single crystal of $[Pd_2Pt_4(\mu_3\text{-}C_7H_7)_4(\text{diphenylacetylene})_2(\text{benzene})(BF_4)][BF_4]$ (**5a'**), which possesses diphenylacetylene ligands at its available Pt sites (Figure 3). The two $PdPt_2$ triangles (dihedral angle = 86.8°) were connected through the Pt1–Pt3 bond (2.6935(2) Å). Thus, the Pt–Pt bond is selectively formed in the dimerization of either Pd_2Pt or $PdPt_2$ sandwich complex. Since the steric environment around the Pt and Pd sites in **2** or **3** can be attributed to be nearly identical, this selectivity might reflect the kinetic or thermodynamic preference of Pt–Pt rather than Pd–Pd or Pd–Pt. The Pt–Pt bond formation might be preferable thermodynamically, as a Pt–Pt bond is usually stronger than a Pd–Pd bond; e.g., the cohesive energy of Pt–Pt (135 kcal/mol) is larger than that of Pd–Pd (90 kcal/mol).[20] The DFT calculations of the model compounds $[Pd_2Pt_4(\mu_3\text{-}C_7H_7)_4(HCN)_4]^{2+}$ (**5''-PtPt**, Pt–Pt coupled dimer; **5''-PdPd**, Pd–Pd coupled dimer) using M06 functional supported the thermodynamic preference of the Pt–Pt coupling over the Pd–Pd coupling [**5''-PtPt** is more stable than **5''-PdPd** by ΔG (298.15 K, 1 atm) = 11.4 kcal/mol].

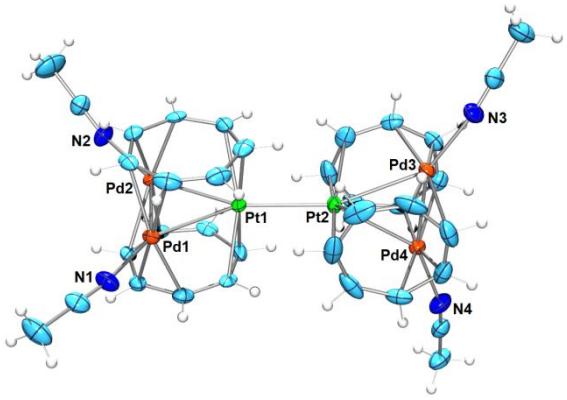

Figure 1. ORTEP of $[Pd_4Pt_2(\mu_3\text{-}C_7H_7)_4(CH_3CN)_4][BF_4]_2$ (**4**) (50% probability ellipsoids, counter anions are omitted for clarity). Selected bond lengths (Å) and angles (deg): Pt1–Pd2 2.8132(5), Pt1–Pd1 2.7931(6), Pd1–Pd2 2.7034(7), Pt1–Pt2 2.6793(3), Pt2–Pd4 2.8449(6), Pt2–Pd3 2.7984(5), Pd3–Pd4 2.6850(7), Pd1–Pd2–Pt1 60.797(15), Pd1–Pt1–Pd2 57.659(15), Pd1–Pt1–Pt2 149.118(15).

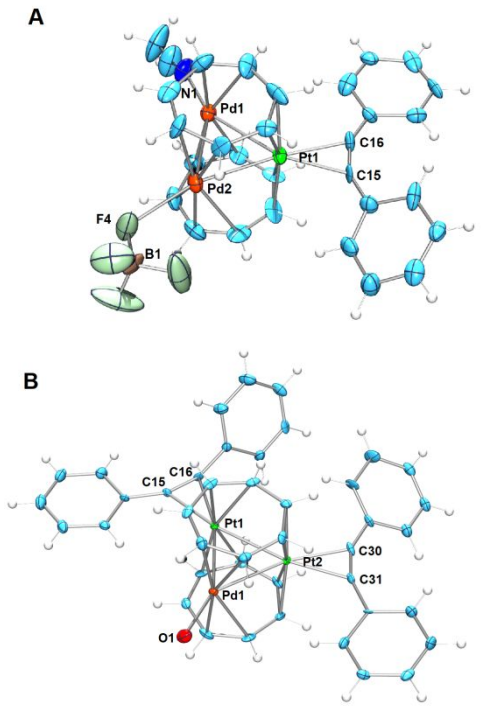

Figure 2. (**A**) ORTEP of $[Pd_2Pt(\mu_3\text{-}C_7H_7)_2(PhC{\equiv}CPh)(CH_3CN)(BF_4)][BF_4]$ (**2a'**) (30% probability ellipsoids, counter anion is omitted for clarity). Selected bond lengths (Å): Pd1–Pd2 2.750(3), Pd1–Pt1 2.791(2), Pd2–Pt1 2.714(3). (**B**) ORTEP of $[PdPt_2(\mu_3\text{-}C_7H_7)_2(PhC{\equiv}CPh)_2(H_2O)][BF_4]_2$ (**3a'**) (30% probability ellipsoids, counter anion is omitted for clarity). Selected bond lengths (Å): Pt1–Pt2 2.7691(7), Pd1–Pt1 2.7950(11), Pd1–Pt2 2.7405(11).

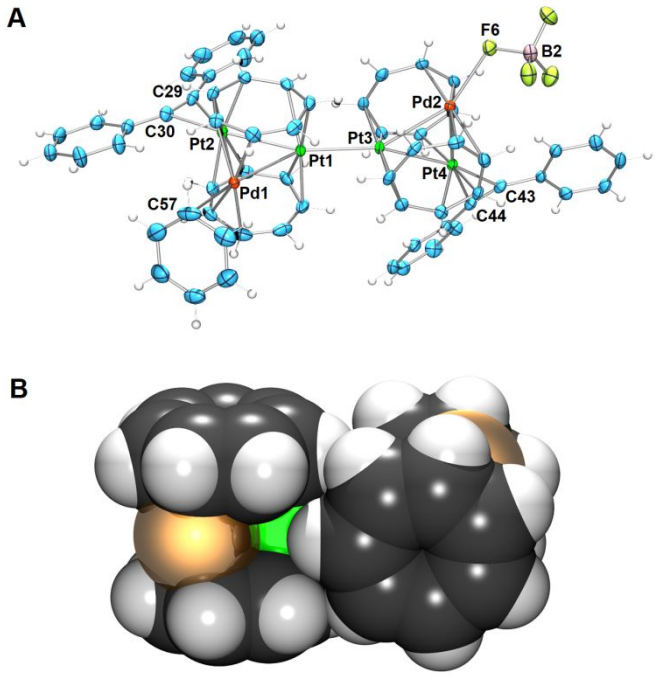

Figure 3. (**A**) ORTEP of $[Pd_2Pt_4(\mu_3\text{-}C_7H_7)_4(diphenylacetylene)_2(benzene)(BF_4)][BF_4]$ (**5a'**) (50% probability ellipsoids, counter anions and solvent molecules are omitted for clarity). Selected bond lengths (Å) and angles (deg): Pt1–Pt2 2.7891(2), Pt1–Pd1 2.8540(3), Pd1–Pt2 2.7324(4), Pt1–Pt3 2.6935(2), Pt3–Pt4 2.7925(2), Pt3–Pd2 2.8325(4), Pd2–Pt4 2.6889(4), Pd1–Pt2–Pt1 62.240(8), Pd1–Pt1–Pt2 57.906(8), Pd1–Pt1–Pt3 148.156(9). (**B**) A space-filling view of the dicationic part of **5a'** (the equatorial ligands are omitted for clarity).

The molecular structures of **4** and **5a'** also suggested that the rotation at the central Pt–Pt bond might be restricted due to the close proximity of the four C_7H_7 ligands (Figure 3B). This restricted rotation was confirmed by the NMR analysis. In solution, the Pd_2Pt dimer **4** showed a sharp singlet resonance (δ 3.85 ppm in CD_3CN) with a ^{195}Pt satellite doublet resonance ($J_{Pt\text{-}H}$ = 8.8 Hz) for the C_7H_7 protons at room temperature (Figure 4, top). In contrast, the $PdPt_2$ dimer **5** exhibited two singlet resonances for the C_7H_7 ligands (δ 3.95 ppm, 3.74 ppm in CD_3CN) (Figure 4, bottom). Raising the temperature up to 75 °C in CD_3CN showed no apparent change of these two resonances of **5**. Such different ^1H NMR signal patterns of **4** and **5** is reasonably explained by considering that the rotation about the Pt–Pt bond connecting the trinuclear sandwich monomer units is slow in the NMR time scale. In **5**, the slow rotation of the central Pt–Pt bond gives an axially chiral structure, where the two C_7H_7 ligands of each monomer unit are chemically non-equivalent with each other, giving two C_7H_7 resonances. The chiral structure of **5** is further supported by the NMR analysis of the tetrakis-dimenylphenylphosphine complex $[Pd_2Pt_4(\mu_3\text{-}C_7H_7)_4(PMe_2Ph)_4][BF_4]_2$ (**5b**) which was generated in CD_3CN by addition of PMe_2Ph (4 equiv) to **5**. The appearance of four resonances for the methyl protons of **5b** can be explained by considering that each PMe_2Ph ligand at the Pd- or Pt site of the chiral cluster framework exhibits two diastereotopic methyl resonances (Figure 5). Thus, the single-crystal X-ray analysis as well as the solution NMR study showed that the $PdPt_2$ sandwich dimer **5** is an axially chiral cluster derived from the arrangement of Pd and Pt atoms in the bi-triangle metal cluster skeleton. The bi-heteroaryl compounds in which the arrangement of hetero-atoms in the skeleton lead to axial chirality are known, as exemplified by the 3,3'-bicollidine (Scheme 3).[21] The present case may represent a rare example that the arrangement of different metal atoms in a mixed metal cluster gives an axially chiral structure. Further studies on the reductive chemistry of mixed-metal sandwich complexes are ongoing in our laboratory.

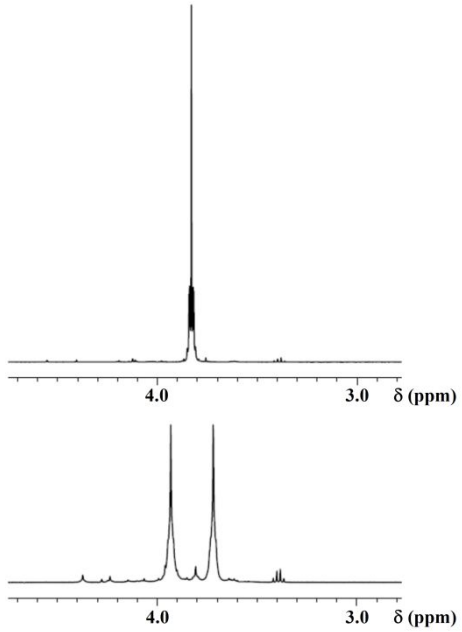

Figure 4. ^{1}H NMR spectra of **4** (top) and **5** (bottom) in CD_3CN at 25 °C.

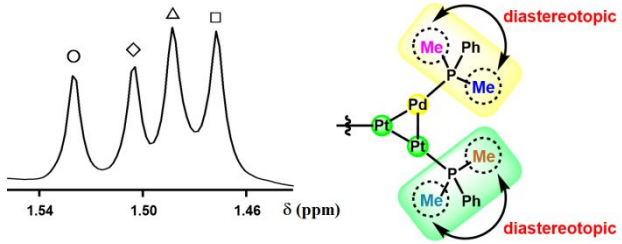

Figure 5. A ^{1}H NMR spectrum of **5b** (CD_3CN, r.t.) exhibiting four resonances for methyl protons.

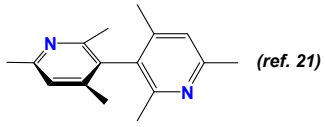

Arrangement of N and C in an Organic Skeleton

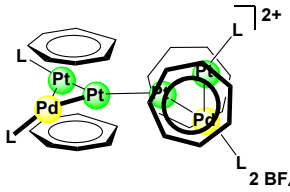

Arrangement of Pd and Pt in a Metal Skeleton

Scheme 3. 3,3'-Collidine (ref. 21) and the present heterometallic sandwich dimer, which are featured by the axially chiral structure derived from atom-arrangement in its main skeleton.

We thank Prof. S. Sakaki (Kyoto University) for helpful discussions. This work was supported by JST-CREST (JPMJCR20B6), JSPS Grant-in-aid for Scientific Research (JP18H01993, JP20H04805, JP20K21205, JP19H04565), and Mitsubishi Foundation.

Notes and references

1 G. Wilkinson, M. Rosenblum, M. C. Whiting, R. B. Woodward, *J. Am. Chem. Soc.* 1952, **74**, 2125.
2 V. V. Strelets, *Coord. Chem. Rev.* 1992, **114**, 1.
3 W. E. Geiger, *Organometallics* 2007, **26**, 5738.
4 M. Malischewski, M. Adelhardt, J. Sutter, K. Meyer, K. Seppelt, *Science*, 2016, **353**, 678.
5 M. J. Chalkley, P. Garrido-Barros, J. C. Peters, *Science*, 2020, **369**, 850.
6 C. A. P. Goodwin, M. J. Giansiracusa, S. M. Greer, H. M. Nicholas, P. Evans, M. Vonci, S. Hill, N. F. Chilton, D. P. Mills, *Nature Chem.* 2021, **13**, 243.
7 M. G. Walawalkar, P. Pandey, R. Murugavel, *Angew. Chem. Int. Ed.* 2021, **60**, 12632.
8 R. L. N. Hailes, A. M. Oliver, J. Gwyther, G. R. Whittell, I. Manners, *Chem. Soc. Rev.* 2016, **45**, 5358.
9 M. S. Inkpen, S. Scheerer, M. Linseis, A. J. P. White, R. F. Winter, T. Albrecht, N. J. Long, *Nature Chem.* 2016, **8**, 825.
10 T. Fukino, H. Joo, Y. Hisada, M. Obana, H. Yamagishi, T. Hikima, M. Takata, N. Fujita, T. Aida, *Science* 2014, **344**, 499.
11 M. W. Droege, W. D. Harman, H. Taube, *Inorg. Chem.* 1987, **26**, 1309.
12 U. T. Mueller-Westerhoff, A. L. Rheingold, G. F. Swiegers, *Angew. Chem. Int. Ed.* 1992, **31**, 1352.
13 a) S. Trupia, A. Nafady, W. E. Geiger, *Inorg. Chem.* 2003, **42**, 5480. b) J. C. Swarts, A. Nafady, J. H. Roudebush, S. Trupia, W. E. Geiger, *Inorg. Chem.* 2009, **48**, 2156.
14 T. Murahashi, Y. Hashimoto, K. Chiyoda, M. Fujimoto, T. Uemura, R. Inoue, S. Ogoshi, H. Kurosawa, *J. Am. Chem. Soc.* 2008, **130**, 8586.
15 T. Murahashi, K. Shirato, A. Fukushima, K. Takase, T. Suenobu, S. Fukuzumi, S. Ogoshi, H. Kurosawa, *Nature Chem.* 2012, **4**, 52.
16 a) E. O. Fischer, H. Wawersik, *J. Organomet. Chem.* 1966, **5**, 559. b) N. El Murr, J. E. Sheats, W. E. Geiger, J. D. L. Holloway, *Inorg. Chem.* 1979, **18**, 1443. c) O. V. Gusev, M. G. Peterleitner, M. A. Ievlev, A. M. Kal'sin, P. V. Petrovskii, L. I. Denisovich, N. A. Ustynyuk, *J. Organomet. Chem.* 1997, **531**, 95. d) S. K. Mohapatra, A. Fonari, C. Risko, K. Yesudas, K. Moudgil, J. H. Delcamp, T. V. Timofeeva, J.-L. Brédas, S. R. Marder, S. Barlow, *Chem. Eur. J.* 2014, **20**, 15385.
17 a) T. Murahashi, M. Fujimoto, M. Oka, Y. Hashimoto, T. Uemura, Y. Tatsumi, Y. Nakao, A. Ikeda, S. Sakaki, H. Kurosawa, *Science* 2006, **313**, 1104. b) F. L. Mulligan, D. C. Babbini, I. R. Davis, S. K. Hurst, G. S. Nichol, *Inorg. Chem.* 2009, **48**, 2708. c) C. Jandl, J. R. Pankhurst, J. B. Love, A. Pöthig, *Organometallics* 2017, **36**, 2772. d) M. Teramoto, K. Iwata, H. Yamaura, K. Kurashima, K. Miyazawa, Y. Kurashige, K. Yamamoto, T. Murahashi, *J. Am. Chem. Soc.* 2018, **140**, 12682.
18 T. Murahashi, K. Usui, R. Inoue, S. Ogoshi, H. Kurosawa, *Chem. Sci.* 2011, **2**, 117.
19 T. Murahashi, K. Usui, Y. Tachibana, S. Kimura, S. Ogoshi, *Chem. Eur. J.* 2012, **18**, 8886.
20 A. De Clercq, S. Giorgio, C. Mottet, *J. Phys.: Condens. Matter* 2016, **28**, 064006.
21 S. Rizzo, S. Arnaboldi, V. Mihali, R. Cirilli, A. Forni, A. Gennaro, A. A. Isse, M. Pierini, P. R. Mussini, F. Sannicolò, *Angew. Chem. Int. Ed.* 2017, **56**, 2079.